The Oxygen-Rich Carboxide Series: CO_n ($n = 3, 4, 5, 6, 7,$ or 8)

Ben M. Elliott and Alexander I. Boldyrev*

Department of Chemistry and Biochemistry, Utah State University, Logan, Utah 84322-0300

Received: November 4, 2004; In Final Form: February 15, 2005

The lowest-energy isomers of the high-order carboxide series, CO_n ($n = 3-8$), have been elucidated via ab initio quantum chemical calculations. The structures of the lowest order of these (3 and 4) are in close agreement with previous calculations and with experimental data. The structures of the higher-order species are elucidated and correlated to the previous structures, showing similarities in structure and reactivity pathways. The reaction energies of the formation of all products are shown to be related. Exothermic pathways of formation often involve a C_{2v} form of CO_2, which was shown to be metastable. The newly identified species could be intermediates in atmospheric reactions. The calculated vibrational frequencies and IR intensities may be used to identify these metastable species.

Introduction

Over the past few decades, there has been continual interest in high-order carboxides, CO_n ($n > 2$). Atmospheric studies in particular have been in the forefront of the research surrounding these species.[1,2] The lowest order of these species, CO_3, has been shown to be a key intermediate in reactions involving mono- and diatomic oxygen with low-order carboxides and organic molecules.[3]

High-order oxides of the group 12 elements would necessarily be highly energetic and, if they could be determined as metastable, would be very likely candidates for high-energy density materials (HEDMs).[4] Wright et al. showed that high-order hydrogen oxides (HO_nH, with $n = 3-5$) could be a promising area of further research.[5] The group of Plesničar[6,7] and our own group[8] characterized the $HOOO^-$ species, which may be a precursor to oxygen dense compounds. Adamantidies et al.[9] theoretically predicted the covalently bound cyclic (D_{2d}) form of O_4. Further theoretical effort occurred as this cyclic O_4 was ~5.3 eV higher in energy than two separate O_2 molecules.[10−14] A D_{3h} form of O_4 analogous to SO_3 was found at a substantially higher energy, 6.5 eV.[15,16] We have shown previously that charged, covalently bound tetra-oxygen O_4^{2-} (C_{3v},$^1A_1$) and O_4^{2+} (D_{4h}, $^1A_{1g}$) and penta-oxygen O_5^{2-} species may be good candidates for oxygen-rich compounds.[17−19]

Studies have been done on silicon oxide clusters,[20,21] which show that this is a prospective area for further research. The C_{2v} cyclic isomer of CO_2 was found to be quite rigid and metastable with respect to the more common linear form.[22] This gives the impression that structures based on a central carbon and bound oxygen rings may be feasible. The CO_3 molecule was much earlier trapped at temperatures of ~100 K.[23,24] Recent theoretical studies were done on CO_3[25,26] and CO_4,[26−30] involving calculations at various levels of theory. Previous works predicted a C_{2v} isomer (Figure 1a) for CO_3,[25,26] which was in close agreement with those earlier low-temperature experiments. For the CO_4 molecule, two low-lying isomers (Figure 1b,c) were found as minima on the potential energy surface (PES).[26−29] Cacace and co-workers recently reported the experimental detection of this CO_4 molecule.[30] They surmised, based upon their own and previous theoretical studies, that the lower-energy isomer, Figure 1b, would proceed to dissociation without a barrier, and that the D_{2d} structure, Figure 1c, would thus be the one observed. This work shows that this is a truly metastable molecule and is attractive for further research.

Herein, we describe the results of our ab initio investigation of the high-order carboxide series, CO_n ($n = 3-8$). Using high-level quantum chemical calculations, we report the geometries, stabilities, and harmonic frequencies of global minima and low-lying isomers of each of these species.

Computational Procedure

All calculations were performed using the Gaussian 03[31] quantum chemical program package. The structures were visualized using the Molden 3.4[32] molecular modeling program. The species' geometries were first optimized, and frequencies were calculated using the hybridized B3LYP[33−35] method as the basic level of calculation with the split-valence 6-311+G*[37−39] basis sets. Structures were then refined using the CCSD(T)[39−41] method with the same basis sets. The appropriateness of the one-electron approximation methods was checked by using the CASSCF[42,43] method with varying active-space sizes and the 6-311+G* basis to calculate geometries and harmonic frequencies.

Results and Discussion

CO_3. The lowest-energy optimized structure is shown in Figure 1 (structure a), and it is a true local minimum. The optimized geometrical parameters and frequencies calculated at the various levels of theory are given in Table 1. Our results agree well with formerly published data.[22−26]

The C_{2v}, $^1A_1$ structure, at the CCSD(T) level of theory, has two C−O distances: the first is 1.18 Å, consistent with a C−O double bond, and the second is 1.33 Å, consistent with C−O single bonds. The O2−O3 distance, 1.65 Å, is somewhat

---

* To whom correspondence should be addressed. E-mail: Boldyrev@cc.usu.edu.

10.1021/jp0449455 CCC: $30.25

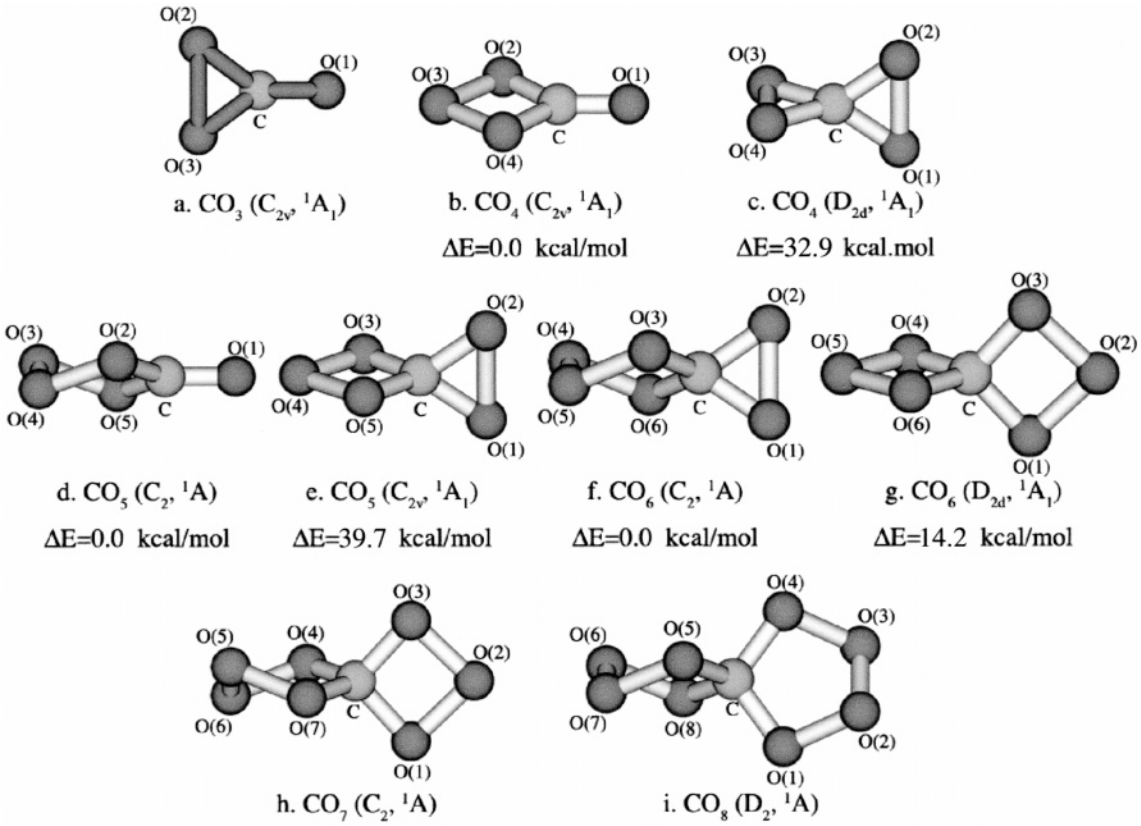

a. CO_3 (C_{2v}, $^1A_1$)

b. CO_4 (C_{2v}, $^1A_1$) ΔE=0.0 kcal/mol

c. CO_4 (D_{2d}, $^1A_1$) ΔE=32.9 kcal.mol

d. CO_5 (C_2, ^1A) ΔE=0.0 kcal/mol

e. CO_5 (C_{2v}, $^1A_1$) ΔE=39.7 kcal/mol

f. CO_6 (C_2, ^1A) ΔE=0.0 kcal/mol

g. CO_6 (D_{2d}, $^1A_1$) ΔE=14.2 kcal/mol

h. CO_7 (C_2, ^1A)

i. CO_8 (D_2, ^1A)

Figure 1. Structures of global minima and low-lying isomers of the CO_n ($n = 3, 4, 5, 6, 7$, or 8) series. The relative energies are given at the CCSD(T)/6-311+G* level of theory.

TABLE 1: Calculated Molecular Properties of CO_3

molecular parameter	B3LYP/ 6-311+G*	CASSCF(8,8)/ 6-311+G*	CCSD(T)/ 6-311+G*
	CO_3 (C_{2v}, $^1A_1$)		
E, au	−263.730 91	−262.514 11 {0.953}[b]	−263.149 65
$R(C-O_1)$, Å	1.17	1.15	1.18
$R(C-O_{2,3})$, Å	1.33	1.31	1.33
$R(O_2-O_3)$, Å	1.59	1.66	1.65
$\omega_1(a_1)$, cm^{-1}	2076 (631.1)[a]	2082	
$\omega_2(a_1)$, cm^{-1}	1122 (15.0)	1145	
$\omega_3(a_1)$, cm^{-1}	680 (12.9)	588	
$\omega_4(b_2)$, cm^{-1}	929 (74.6)	952	
$\omega_5(b_2)$, cm^{-1}	571 (6.4)	600	
$\omega_6(b_1)$, cm^{-1}	669 (35.2)	759	

[a] The values in parentheses represent the intensities (km/mol) of IR active vibrational modes. [b] The values in braces indicate C_{HF} values in the CASSCF expansion.

TABLE 2: Calculated Molecular Properties of CO_4

molecular parameter	B3LYP/ 6-311+G*	CASSCF(8,8)/ 6-311+G*	CCSD(T)/ 6-311+G*
	CO_4 (C_{2v}, $^1A_1$)		
E, au	−338.904 47	−337.305 97 {0.978}[b]	−338.155 77
$R(C-O_1)$, Å	1.17	1.15	1.18
$R(C-O_2)$, Å	1.37	1.34	1.37
$R(O_2-O_3)$, Å	1.46	1.50	1.48
$\angle(O_2-C-O_4)$, deg	95.5	98.0	96.5
$\omega_1(a_1)$, cm^{-1}	1996 (599.4)[a]	2073	
$\omega_2(a_1)$, cm^{-1}	1033 (42.4)	1189	
$\omega_3(a_1)$, cm^{-1}	912 (0.4)	1165	
$\omega_4(a_1)$, cm^{-1}	789 (13.5)	888	
$\omega_5(b_2)$, cm^{-1}	1116 (113.8)	1180	
$\omega_6(b_2)$, cm^{-1}	866 (1.0)	1161	
$\omega_7(b_2)$, cm^{-1}	513 (3.5)	455	
$\omega_8(b_1)$, cm^{-1}	722 (24.2)	791	
$\omega_9(b_1)$, cm^{-1}	298 (1.5)	306	
	CO_4 (D_{2d}, $^1A_1$)		
E, au	−338.841 36	−337.308 67 {0.896}[b]	−338.103 40
$R(C-O_1)$, Å	1.34	1.33	1.34
$R(O_1-O_2)$, Å	1.56	1.68	1.61
$\omega_1(b_2)$, cm^{-1}	1670 (487.8)	1718	
$\omega_2(b_2)$, cm^{-1}	753 (16.8)	458	
$\omega_3(a_1)$, cm^{-1}	1034 (0)	978	
$\omega_4(a_1)$, cm^{-1}	606 (0)	422	
$\omega_6(e)$, cm^{-1}	1005 (49.3)	1186	
$\omega_7(e)$, cm^{-1}	540 (12.5)	590	
$\omega_8(b_1)$, cm^{-1}	345 (0)	376	

[a] The values in parentheses represent the intensities (km/mol) of IR active vibrational modes. [b] The values in braces indicate C_{HF} values in the CASSCF expansion.

overlong for an O−O single bond but may be tentatively attributed to the strain of the three corniced ring structure and the repulsion of the electrons on the electron-rich oxygens. The Hartree−Fock configuration is dominant in the CASSCF(8,8) wave function ($C_{HF} = 0.953$), indicating that our results based on the single-determinant methods (B3LYP and CCSD(T)) are reliable.

Although CO_3 is not stable against dissociation into CO_2 and O, at the B3LYP level of theory, the reaction of CO with O_2 exothermically yields CO_3 (C_{2v}, $^1A_1$). At the highest level of theory (CCSD(T)), the value is again exothermic with a fair amount of released energy.

$$\mathrm{CO}\ (C_{\infty v},\ ^1\Sigma^+) + \mathrm{O_2}\ (D_{\infty h},\ ^3\Sigma_g^-) \rightarrow \mathrm{CO_3}\ (C_{2v},\ ^1A_1) \qquad \Delta E = -13.9\ \text{kcal/mol} \quad (1)$$

(All energy values for reaction pathways are given at the CCSD(T)/6-311+G* level of theory.)

CO_4. The lowest-energy optimized structures and relative energies are shown in Figure 1 (structures b and c). The optimized geometrical parameters and frequencies calculated at the various levels of theory are given in Table 2.

Concurrent with previous works,[26−30] we find two isomers being local minima, with the C_{2v}, $^1A_1$ isomer of CO_4 lying 30.8 kcal/mol below the D_{2d}, $^1A_1$ isomer at the B3LYP level and 32.9 kcal/mol below it at the CCSD(T) level of theory. This energy difference could be attributed to the lack of π character to the bonding in the D_{2d} isomer as well as less ring strain in the four-membered ring of the C_{2v} isomer compared to the three-membered rings in the D_{2d} isomer. The Hartree−Fock configuration is again dominant in the CASSCF expansion for both structures (C_{HF} (C_{2v}) = 0.978, C_{HF} (D_{2d}) = 0.896).

These structures are both unstable with respect to dissociation into CO_2 and O_2 but are stable with respect to CO and O_3, as well as CO_3 and O.

$$CO_2\ (D_{\infty h},\ ^1\Sigma_g^+) + O_2\ (D_{\infty h},\ ^3\Sigma_g^-) \rightarrow CO_4\ (C_{2v},\ ^1A_1) \quad \Delta E = 69.35\ \text{kcal/mol} \quad (2)$$

$$CO_2\ (D_{\infty h},\ ^1\Sigma_g^+) + O_2\ (D_{\infty h},\ ^3\Sigma_g^-) \rightarrow CO_4\ (D_{2d},\ ^1A_1) \quad \Delta E = 102.22\ \text{kcal/mol} \quad (3)$$

$$CO\ (C_{\infty v},\ ^1\Sigma^+) + O_3\ (C_{2v},{}^1A_1) \rightarrow CO_4\ (C_{2v},\ ^1A_1) \quad \Delta E = -44.61\ \text{kcal/mol} \quad (4)$$

$$CO\ (C_{\infty v},\ ^1\Sigma^+) + O_3\ (C_{2v},{}^1A_1) \rightarrow CO_4\ (D_{2d},\ ^1A_1) \quad \Delta E = -11.74\ \text{kcal/mol} \quad (5)$$

$$CO_3\ (C_{2v},\ ^1A_1) + O\ (^3P) \rightarrow CO_4\ (C_{2v},\ ^1A_1) \quad \Delta E = -42.65\ \text{kcal/mol} \quad (6)$$

$$CO_3\ (C_{2v},{}^1A_1) + O\ (^3P) \rightarrow CO_4\ (D_{2d},\ ^1A_1) \quad \Delta E = -9.78\ \text{kcal/mol} \quad (7)$$

CO_5. The lowest-energy optimized structures and relative energies are shown in Figure 1 (structures d and e). The optimized geometrical parameters and frequencies calculated at the various levels of theory are given in Table 3. No previous work could be found on these species according to the best of our knowledge.

Further addition of oxygen to the proposed series reveals two minima on the potential energy surface. The trend seen in the previous species is continued here. The lowest-energy isomer (Figure 1d) shows the characteristic doubly bonded oxygen opposite a five-membered ring. The bond lengths in the ring, at the CCSD(T) level, again correspond to typical C−O (1.38 Å) and O−O (1.46/1.42 Å) single bonds. The slightly increased energy difference (ΔE = 38.74 kcal/mol, CCSD(T) level) between the two structures would probably correspond to the reduced ring strain of the five-membered ring and the energetics of the C−O double bond. Again, the Hartree−Fock configuration is dominant with C_{HF} (C_2) = 0.949 and C_{HF} (C_{2v}) = 0.901.

TABLE 3: Calculated Molecular Properties of CO_5

molecular parameter	B3LYP/ 6-311+G*	CASSCF(8,8)/ 6-311+G*	CCSD(T)/ 6-311+G*
	CO_5 (C_2, ^1A)		
E, au	−414.072 33	−412.140 91 {0.949}[b]	−413.160 30
$R(C-O_1)$, Å	1.18	1.18	1.18
$R(C-O_2)$, Å	1.38	1.35	1.38
$R(O_2-O_4)$, Å	1.45	1.41	1.46
$R(O_3-O_4)$, Å	1.41	1.46	1.42
$\angle(O_2-C-O_5)$, deg	109.2	109.0	109.5
$\angle(C-O_2-O_4)$, deg	103.8	104.9	103.6
$\angle(C-O_2-O_4-O_3)$, deg	−38.3	−38.6	−38.3
ω_1(a), cm^{-1}	1929 (479.7)[a]	1980	
ω_2(a), cm^{-1}	939 (21.7)	1100	
ω_3(a), cm^{-1}	886 (47.0)	1028	
ω_4(a), cm^{-1}	762 (18.6)	971	
ω_5(a), cm^{-1}	668 (6.7)	708	
ω_6(a), cm^{-1}	389 (1.5)	407	
ω_7(b), cm^{-1}	1092 (131.1)	1324	
ω_8(b), cm^{-1}	867 (9.1)	810	
ω_9(b), cm^{-1}	745 (18.3)	790	
ω_{10}(b), cm^{-1}	696 (14.0)	765	
ω_{11}(b), cm^{-1}	490 (3.9)	529	
ω_{12}(b), cm^{-1}	198 (0.6)	178	
	CO_5 (C_{2v}, $^1A_1$)		
E, au	−414.000 90	−412.107 13 {0.901}[b]	−413.098 57
$R(C-O_{1,2})$, Å	1.35	1.34	1.35
$R(C-O_{3,5})$, Å	1.38	1.36	1.38
$R(O_{3,5}-O_4)$, Å	1.47	1.52	1.49
$\angle(O_1-C-O_2)$, deg	70.4	76.4	72.9
$\angle(O_3-C-O_5)$, deg	95.6	98.5	96.5
ω_1(a_1), cm^{-1}	1495 (512.6)	1608	
ω_2(a_1), cm^{-1}	994 (36.7)	1052	
ω_3(a_1), cm^{-1}	930 (5.5)	752	
ω_4(a_1), cm^{-1}	837 (19.5)	710	
ω_5(a_1), cm^{-1}	590 (0.5)	463	
ω_6(b_1), cm^{-1}	1147 (67.6)	1351	
ω_7(b_1), cm^{-1}	908 (4.7)	734	
ω_8(b_1), cm^{-1}	487 (6.4)	529	
ω_9(b_2), cm^{-1}	958 (50.5)	1161	
ω_{10}(b_2), cm^{-1}	556 (5.3)	628	
ω_{11}(b_2), cm^{-1}	173 (0.4)	146	
ω_{12}(a_2), cm^{-1}	284 (0)	350	

[a] The values in parentheses represent the intensities (km/mol) of IR active vibrational modes. [b] The values in braces indicate C_{HF} values in the CASSCF expansion.

As with CO_4, we might suppose that the symmetry rules will allow the C_{2v} isomer to be much longer lived than the C_2 isomer. The formation energies of CO_5 (C_2,^1A) are endothermic via the typical pathways employing well-known molecules. However, the addition of a single oxygen atom to CO_4 and the combination of the C_{2v} isomer of CO_2 with O_3 are both exothermic reactions.

$$CO_2\ (D_{\infty h},\ ^1\Sigma_g^+) + O_3\ (C_{2v},\ ^1A_1) \rightarrow CO_5\ (C_2,{}^1A) \quad \Delta E = 39.65\ \text{kcal/mol} \quad (8)$$

$$CO\ (C_{\infty v},\ ^1\Sigma_g^+) + 2O_2\ (D_{\infty h},\ ^3\Sigma_g^-) \rightarrow CO_5\ (C_2,{}^1A) \quad \Delta E = 7.56\ \text{kcal/mol} \quad (9)$$

$$CO_3\ (C_{2v},{}^1A_1) + O_2\ (D_{\infty h},\ ^3\Sigma_g^-) \rightarrow CO_5\ (C_2,{}^1A) \quad \Delta E = 21.47\ \text{kcal/mol} \quad (10)$$

$$CO_2\ (C_{2v},\ ^1A_1) + O_3\ (C_{2v},\ ^1A_1) \rightarrow CO_5\ (C_2,{}^1A) \quad \Delta E = -102.58\ \text{kcal/mol} \quad (11)$$

$$CO_4\ (C_{2v},\ ^1A_1) + O\ (^3P) \rightarrow CO_5\ (C_2,{}^1A) \quad \Delta E = -41.65\ \text{kcal/mol} \quad (12)$$

CO_6. The lowest-energy optimized structures and relative energies are shown in Figure 1 (structures f and g). The optimized geometrical parameters and frequencies calculated at the various levels of theory are given in Table 4. The Hartree−Fock configurations in the CASSCF expansion (C_{HF}) are 0.930 and 0.963 for the C_2 and D_{2d} isomers, respectively.

In these structures, the trend of favoring the five-membered ring continues. Increased ring size beyond the five-membered ring, however, is not stable. A structure with a six-membered ring opposing a single oxygen−carbon double bond had one imaginary frequency and separated into CO_2 and O_2 upon following the frequency. This, along with the strain of the three-membered ring, makes the difference between the two isomers found to be only 14.2 kcal/mol (CCSD(T) values).

There is a similar situation here in the dissociation energies, as in CO_5. The only exothermic channels involve CO_2 (C_{2v}, $^1A_1$) or O (^3P).

$$CO_2\ (D_{\infty h},\ {}^1\Sigma_g^+) + 2O_2\ (D_{\infty h},\ {}^3\Sigma_g^-) \rightarrow CO_6\ (C_2, {}^1A) \qquad \Delta E = 124.05\ \text{kcal/mol} \quad (13)$$

$$CO\ (C_{\infty v},\ {}^1\Sigma^+) + O_2\ (D_{\infty h},\ {}^3\Sigma_g^-) + O_3\ (C_{2v},\ {}^1A_1) \rightarrow CO_6\ (C_2, {}^1A) \qquad \Delta E = 10.08\ \text{kcal/mol} \quad (14)$$

$$CO_3\ (C_{2v}, {}^1A_1) + O_3\ (C_{2v},\ {}^1A_1) \rightarrow CO_6\ (C_2, {}^1A) \qquad \Delta E = 23.99\ \text{kcal/mol} \quad (15)$$

$$CO_4\ (D_{2d},\ {}^1A_1) + O_2\ (D_{\infty h},\ {}^3\Sigma_g^-) \rightarrow CO_6\ (C_2, {}^1A) \qquad \Delta E = 21.83\ \text{kcal/mol} \quad (16)$$

$$CO_2\ (C_{2v},\ {}^1A_1) + 2O_2\ (D_{\infty h},\ {}^3\Sigma_g^-) \rightarrow CO_6\ (C_2, {}^1A) \qquad \Delta E = -18.18\ \text{kcal/mol} \quad (17)$$

$$CO_5\ (C_{2v}, {}^1A_1) + O\ ({}^3P) \rightarrow CO_6\ (C_2, {}^1A) \qquad \Delta E = -48.16\ \text{kcal/mol} \quad (18)$$

CO_7. The lowest-energy optimized structure is shown in Figure 1 (structure h). The optimized geometrical parameters and frequencies calculated at the various levels of theory are given in Table 5. The Hartree−Fock configuration is still dominant in the CASSCF wave function ($C_{\mathrm{HF}} = 0.966$).

In this system, the only found minimum corresponds to an addition of O to the three-membered ring of the CO_6 C_{2v} isomer, or to one of the four-membered rings of the D_{2d} isomer. The bond lengths are all familiar single O−O and C−O bonds.

The energetics follow the same pattern already seen.

$$CO_2\ (D_{\infty h},\ {}^1\Sigma_g^+) + O_2\ (D_{\infty h},\ {}^3\Sigma_g^-) + O_3\ (C_{2v},\ {}^1A_1) \rightarrow CO_7\ (C_2, {}^1A) \qquad \Delta E = 102.42\ \text{kcal/mol} \quad (19)$$

$$CO_2\ (C_{2v},\ {}^1A_1) + O_2\ (D_{\infty h},\ {}^3\Sigma_g^-) + O_3\ (C_{2v},\ {}^1A_1) \rightarrow CO_7\ (C_2, {}^1A) \qquad \Delta E = \text{-}39.80\ \text{kcal/mol} \quad (20)$$

$$CO_6\ (C_2, {}^1A) + O\ ({}^3P) \rightarrow CO_7\ (C_2, {}^1A) \qquad \Delta E = -33.58\ \text{kcal/mol} \quad (21)$$

CO_8. The lowest-energy optimized structure is shown in Figure 1 (structure i). The optimized geometrical parameters and frequencies calculated at the various levels of theory are given in Table 6. The CASSCF expansion gives a dominant Hartree−Fock configuration ($C_{\mathrm{HF}} = 0.933$) once again.

Again, the only minimum found for this species was the addition of a single O to the previous CO_7 (C_2, ^1A). The bond lengths are all very typical single bond lengths with no ring strain stretching. There are two exothermic pathways, one involving CO_2 (C_{2v}, $^1A_1$) and O_3 (C_{2v}, $^1A_1$) and the other CO_7 and O (^3P).

TABLE 4: Calculated Molecular Properties of CO_6

molecular parameter	B3LYP/ 6-311+G*	CASSCF(8,8)/ 6-311+G*	CCSD(T)/ 6-311+G*
		CO_6 (C_2, ^1A)	
E, au	−489.179 37	−486.854 99 {0.930}[b]	−488.113 47
$R(C-O_{1,2})$, Å	1.35	1.34	1.35
$R(C-O_{3,6})$, Å	1.39	1.37	1.40
$R(O_3-O_5, O_4-O_6)$, Å	1.45	1.36	1.46
$R(O_4-O_5)$, Å	1.40	1.47	1.41
$\angle(O_1-C-O_2)$, deg	69.8	76.1	72.2
$\angle(O_3-C-O_6)$, deg	108.4	106.7	108.5
$\angle(C-O_3-O_5)$, deg	102.4	105.4	102.0
$\angle(O_3-O_5-O_4)$, deg	99.5	98.7	98.9
$\angle(C-O_3-O_5-O_4)$, deg	−42.5	−39.8	−43.7
ω_1(a), cm^{-1}	1460 (376.7)[a]	1590	
ω_2(a), cm^{-1}	948 (12.4)	1209	
ω_3(a), cm^{-1}	883 (48.1)	991	
ω_4(a), cm^{-1}	805 (2.5)	758	
ω_5(a), cm^{-1}	709 (18.5)	656	
ω_6(a), cm^{-1}	544 (5.1)	474	
ω_7(a), cm^{-1}	472 (0.2)	446	
ω_8(a), cm^{-1}	308 (0.5)	338	
ω_9(b), cm^{-1}	1075 (82.8)	1295	
ω_{10}(b), cm^{-1}	987 (43.3)	1204	
ω_{11}(b), cm^{-1}	855 (9.4)	1161	
ω_{12}(b), cm^{-1}	726 (1.1)	826	
ω_{13}(b), cm^{-1}	575 (9.7)	641	
ω_{14}(b), cm^{-1}	446 (3.0)	520	
ω_{15}(b), cm^{-1}	136 (0.4)	135	
		CO_6 (D_{2d}, $^1A_1$)	
E, au	−489.158 18	−486.788 63 {0.963}[c]	−488.090 91
$R(C-O_{1,3,4,6})$, Å	1.39	1.36[c]	1.39
$R(O_{1,3}-O_2, O_{4,6}-O_5)$, Å	1.47	1.44[c]	1.48
$\angle(O_1-C-O_3)$, deg	94.1	94.0[c]	95.2
ω_1(b$_2$), cm^{-1}	1268 (562.0)	1501[c]	
ω_2(b$_2$), cm^{-1}	944 (11.4)	1056[c]	
ω_3(b$_2$), cm^{-1}	880 (31.1)	1041[c]	
ω_4(e), cm^{-1}	1095 (67.5)	1305[c]	
ω_5(e), cm^{-1}	892 (3.1)	943[c]	
ω_6(e), cm^{-1}	500 (2.1)	585[c]	
ω_7(e), cm^{-1}	185 (0.3)	156[c]	
ω_8(a$_1$), cm^{-1}	1002 (0)	1131[c]	
ω_9(a$_1$), cm^{-1}	926 (0)	1042[c]	
ω_{10}(a$_1$), cm^{-1}	549 (0)	617[c]	
ω_{11}(b$_1$), cm^{-1}	214 (0)	329[c]	

[a] The values in parentheses represent the intensities (km/mol) of IR active vibrational modes. [b] The values in braces indicate C_{HF} values in the CASSCF expansion. [c] These values were calculated with the four active electrons and seven active molecular orbitals in the CASSCF expansion.

$$CO_2\ (D_{\infty h},\ {}^1\Sigma_g^+) + 3O_2\ (D_{\infty h},\ {}^3\Sigma_g^-) \rightarrow CO_8\ (D_2, {}^1A) \qquad \Delta E = 145.69\ \text{kcal/mol} \quad (22)$$

$$CO_2\ (C_{2v},\ {}^1A_1) + 3O_2\ (D_{\infty h},\ {}^3\Sigma_g^-) \rightarrow CO_8\ (D_2, {}^1A) \qquad \Delta E = 3.47\ \text{kcal/mol} \quad (23)$$

$$CO_2\ (C_{2v},\ {}^1A_1) + 2O_3\ (C_{2v},\ {}^1A_1) \rightarrow CO_8\ (D_2, {}^1A) \qquad \Delta E = -78.40\ \text{kcal/mol} \quad (24)$$

$$CO_7\ (C_2, {}^1A) + O({}^3P) \rightarrow CO_8\ (D_2, {}^1A) \qquad \Delta E = -50.55\ \text{kcal/mol} \quad (25)$$

TABLE 5: Calculated Molecular Properties of CO_7

molecular parameter	B3LYP/ 6-311+G*	CASSCF(8,8)/ 6-311+G*	CCSD(T)/ 6-311+G*
	CO_7 (C_2, $^1A_1$)		
E, au	−564.334 54	−561.623 09 {0.966}[b]	−563.105 13
$R(C-O_{1,3})$, Å	1.40	1.37	1.40
$R(C-O_{4,7})$, Å	1.40	1.37	1.40
$R(O_{1,3}-O_2)$, Å	1.47	1.39	1.49
$R(O_4-O_6, O_5-O_7)$, Å	1.45	1.40	1.46
$R(O_5-O_6)$, Å	1.40	1.44	1.41
$\angle(O_1-C-O_3)$, deg	94.4	92.0	95.6
$\angle(O_4-C-O_7)$, deg	108.8	106.6	107.1
$\angle(C-O_4-O_6)$, deg	103.3	105.0	102.8
$\angle(O_4-O_6-O_5)$, deg	99.2	98.6	98.7
$\angle(C-O_7-O_5-O_6)$, deg	42.8	41.2	44.1
ω_1(a), cm^{-1}	1221 (463.0)[a]	1464	
ω_2(a), cm^{-1}	977 (1.2)	1190	
ω_3(a), cm^{-1}	932 (0.3)	1134	
ω_4(a), cm^{-1}	919 (11.5)	1060	
ω_5(a), cm^{-1}	833 (30.0)	961	
ω_6(a), cm^{-1}	708 (35.3)	798	
ω_7(a), cm^{-1}	507 (3.6)	564	
ω_8(a), cm^{-1}	455 (0.0)	463	
ω_9(a), cm^{-1}	256 (0.2)	313	
ω_{10}(b), cm^{-1}	1121 (52.3)	1312	
ω_{11}(b), cm^{-1}	1037 (85.5)	1272	
ω_{12}(b), cm^{-1}	909 (4.6)	1187	
ω_{13}(b), cm^{-1}	844 (5.1)	1019	
ω_{14}(b), cm^{-1}	711 (2.3)	811	
ω_{15}(b), cm^{-1}	531 (4.9)	615	
ω_{16}(b), cm^{-1}	465 (0.6)	541	
ω_{17}(b), cm^{-1}	181 (0.6)	175	
ω_{18}(b), cm^{-1}	100 (0.0)	99	

[a] The values in parentheses represent the intensities (km/mol) of IR active vibrational modes. [b] The values in braces indicate C_{HF} values in the CASSCF expansion.

TABLE 6: Calculated Molecular Properties of CO_8

molecular parameter	B3LYP/ 6-311+G*	CASSCF(8,8)/ 6-311+G*	CCSD(T)/ 6-311+G*
	CO_8 (D_2, ^1A)		
E, au	−639.515 27	−636.486 29 {0.933}[b]	−638.123 84
$R(C-O_{1,4,5,8})$, Å	1.41	1.37	1.41
$R(O_1-O_2, O_5-O_7)$, Å	1.45	1.40	1.46
$R(O_2-O_3, O_6-O_7)$, Å	1.40	1.46	1.41
$\angle(O_1-C-O_4)$, deg	107.3	106.8	107.8
$\angle(C-O_1-O_2)$, deg	102.4	104.6	101.9
$\angle(O_1-O_2-O_3)$, deg	99.3	98.2	98.7
$\angle(C-O_1-O_2-O_3)$, deg	−43.4	−42.1	−44.6
$\omega_1(b_2)$, cm^{-1}	1181 (363.8)[a]	1417	
$\omega_2(b_2)$, cm^{-1}	940 (0.6)	1081	
$\omega_3(b_2)$, cm^{-1}	791 (18.3)	915	
$\omega_4(b_2)$, cm^{-1}	669 (85.9)	721	
$\omega_5(b_2)$, cm^{-1}	476 (1.1)	457	
$\omega_6(b_1)$, cm^{-1}	1074 (63.3)	1330	
$\omega_7(b_1)$, cm^{-1}	862 (7.6)	998	
$\omega_8(b_1)$, cm^{-1}	729 (3.7)	807	
$\omega_9(b_1)$, cm^{-1}	445 (0.0)	509	
$\omega_{10}(b_1)$, cm^{-1}	165 (0.5)	139	
$\omega_{11}(b_3)$, cm^{-1}	1018 (80.4)	1253	
$\omega_{12}(b_3)$, cm^{-1}	846 (1.2)	1003	
$\omega_{13}(b_3)$, cm^{-1}	711 (0.6)	802	
$\omega_{14}(b_3)$, cm^{-1}	556 (5.9)	638	
$\omega_{15}(b_3)$, cm^{-1}	83 (0.3)	57	
ω_{16}(a), cm^{-1}	960 (0)	1109	
ω_{17}(a), cm^{-1}	876 (0)	968	
ω_{18}(a), cm^{-1}	719 (0)	740	
ω_{19}(a), cm^{-1}	530 (0)	540	
ω_{20}(a), cm^{-1}	428 (0)	463	
ω_{21}(a), cm^{-1}	269 (0)	294	

[a] The values in parentheses represent the intensities (km/mol) of IR active vibrational modes. [b] The values in braces indicate C_{HF} values in the CASSCF expansion.

Alternative Structures

In the search for the global minimum, we calculated a large number of alternative structures. The CO_n species followed similar patterns until CO_7 was reached, at which point, the relatively low-lying alternative structures disappeared. We found that very few alternative structures for the higher-order species are minima on the potential energy surface. For example, any structure involving a six-membered ring was a saddle point with one imaginary frequency. Following this frequency caused all such species to fall apart into lesser species (e.g., CO_6 becomes $CO_2 + 2O_2$ and CO_8 becomes $CO_4 + 2O_2$). There were a few local minima on the PES. These species, however, proved to be so high on the PES as to be unfeasible. All other attempted species proved to be first-order or higher saddle points on the PES and following the imaginary frequencies led to either the found minima described above or to the dissociated van der Waals species.

Conclusions

We have found the lowest-energy covalently bound minima of the high-order carboxide series, CO_n ($n = 3-8$). The minima are very high-energy species lying far above the ground state of CO_2 ($D_{\infty h}$, $^1\Sigma_g^+$) and O_2 ($D_{\infty h}$, $^3\Sigma_g^-$) and thus could be viable only as metastable species. There are few pathways for these species that would lead to them exothermically. However, we have shown that the use of CO_2 (C_{2v}, $^1A_1$), which was shown to be a metastable higher-energy isomer of CO_2, for most of these species leads favorably to the desired products in the gas phase. The harmonic frequencies could be used be used for identifying the hyper-oxygen species, either under matrix isolation or in the gas phase under certain conditions. We hope that this research will lead to a broader view of the chemistries possible for high-order oxygen species.

Acknowledgment. This work was made possible by funds from the PRF administered by the ACS (ACS-PRF 38242-AC6).

References and Notes

(1) (a) Narcisi, R. S.; Bailey, A. D.; Della Lucca, L.; Sherman, C.; Thomas, D. M. *J. Atmos. Terr. Phys.* **1971**, *33*, 1174. (b) Arnold, F.; Viggiano, A. A.; Ferguson, E. E. *Planet. Space Sci.* **1982**, *30*, 1317. (c) Wisemberg, J.; Kockarts, G. *J. Geophys. Res.* **1980**, *85*, 4642. (d) Thomas, L.; Bowman, M. R. *J. Atmos. Terr. Phys.* **1985**, *47*, 547. (e) Viggiano, A. A.; Morris, R. A.; Paulson, J. F. *J. Chem. Phys.* **1989**, *91*, 5855. (f) Dymek, M. K. *Adv. Space Explor.* **1980**, *8*, 115. (g) Wayne, R. P. *Chemistry of Atmospheres*; Oxford University Press: Oxford, U.K., 2000.

(2) (a) Keating, G. M., Ed. *Adv. Space Res.* **1990**, *10*, No. 5. (b) Fox, J. L. *Icarus* **1982**, *51*, 248. (c) Hashimoto, G. L.; Abe, Y.; Sasaki, S. *Geophys. Res. Lett.* **1997**, *24*, 289.

(3) Parnis, J. M.; Hoover, L. E.; Fridgen, T. D.; Lafleur, R. D. *J. Phys. Chem.* **1993**, *97*, 10708.

(4) (a) Shields, H.; Smith, A. L. S. *Appl. Phys.* **1978**, *16*, 111. (b) Scott, W. B. *Aviat. Week Space Technol.* **1988**, *21*, 19. (c) Klapötke, T. M.; Holl, G. *Green Chem.* **2001**, *3*, G75.

(5) Mckay, D. J.; Wright, J. S. *J. Am. Chem. Soc.* **1998**, *120*, 1003.

(6) Kraka, E.; Cremer, D.; Koller, J.; Plesničar, B. *J. Am. Chem. Soc.* **2002**, *124*, 8462.

(7) Plesničar, B.; Cerkovnik, J.; Tuttle, T.; Kraka, E.; Cremer, D. *J. Am. Chem. Soc.* **2002**, *124*, 11260.

(8) Elliott, B.; Alexandrova, A. N.; Boldyrev, A. I. *J. Phys. Chem. A* **2003**, *107*, 1203.

(9) Adamantidies, V.; Neisius, D.; Verhaegen, G. *Chem. Phys.* **1980**, *48*, 215.

(10) Campargue, A.; Biennier, L.; Kachanov, A.; Jost, R.; Bussery-Honvault, B.; Veyret, V.; Churassy, S.; Bacis, R. *Chem. Phys. Lett.* **1988**, *288*, 734.

(11) Aquilanti, V.; Ascenzi, D.; Bartolomei, M.; Cappelletti, D.; Cavalli, S.; de Castro Vitores, M.; Pirani, F. *Phys. Rev. Lett.* **1999**, *82*, 69.

(12) Peterka, D. S.; Ahmed, M.; Suits, A. G.; Wilson, K. J.; Korkin, A.; Nooijen, M.; Bartlett, R. J. *J. Chem. Phys.* **1999**, *110*, 6095.

(13) Seidl, E. T.; Schaefer, H. F. *J. Chem. Phys.* **1988**, *88*, 7043; **1992**, *96*, 1176.

(14) Dunn, K. M.; Scuseria, G. E.; Schaefer, H. F. *J. Chem. Phys.* **1990**, *92*, 6077.

(15) Roeggen, I.; Nilssen, E. W. *Chem. Phys. Lett.* **1989**, *157*, 409.

(16) Hottoka, M.; Pyykko, P. *Chem. Phys. Lett.* **1989**, *157*, 415.

(17) Zhai, H.-J.; Yang, X.; Wang, X.-B.; Wang, L.-S.; Elliott, B.; Boldyrev, A. I. *J. Am. Chem. Soc.* **2002**, *124*, 6742.

(18) Elliott, B. M.; Boldyrev, A. I. *Inorg. Chem.* **2004**, *43*, 4109.

(19) Elliott, B. M.; Boldyrev, A. I. *J. Phys. Chem. A* **2005**, *109*, 236.

(20) Chu, T. S.; Zhang, R. Q.; Cheung, H. F. *J. Phys. Chem. B* **2001**, *105*, 1705.

(21) Lu, W. C.; Wang, C. Z.; Nguyen, V.; Schmidt, M. W.; Gordon, M. S.; Ho, K. M. *J. Phys. Chem. A* **2003**, *107*, 6936.

(22) Xantheas, S. S.; Ruedenberg, K *Int. J. Quantum Chem.* **1994**, *49*, 409 and references therein.

(23) Weissberger, E.; Breckenridge, W. H.; Taube, H. *J. Chem. Phys.* **1967**, *47*, 1764.

(24) Jacox, M. E.; Milligan, D. E. *J. Chem. Phys.* **1971**, *54*, 919.

(25) Froese, R. D. J.; Goddard, J. D. *J. Phys. Chem.* **1993**, *97*, 7484.

(26) Averyanov, A. S.; Khait, Y. G.; Puzanov, Y. V. *THEOCHEM* **1999**, *459*, 95.

(27) Averyanov, A. S.; Khait, Y. G.; Puzanov, Y. V. *THEOCHEM* **1996**, *367*, 87.

(28) Song, J.; Khait, Y. G.; Hoffmann, M. R. *J. Phys. Chem. A* **1999**, *103*, 521.

(29) Korkin, A. A.; Schleyer, P. v. R.; Boyd, R. J. *Chem. Phys. Lett.* **1994**, *227*, 312.

(30) Cacace, F.; Petris, G. d.; Rosi, M.; Troiani, A. *Angew. Chem., Int. Ed.* **2003**, *42*, 2985.

(31) Frisch, M. J.; Trucks, G. W.; Schlegel, H. B.; Scuseria, G. E.; Robb, M. A.; Cheeseman, J. R.; Montgomery, J. A., Jr.; Vreven, T.; Kudin, K. N.; Burant, J. C.; Millam, J. M.; Iyengar, S. S.; Tomasi, J.; Barone, V.; Mennucci, B.; Cossi, M.; Scalmani, G.; Rega, N.; Petersson, G. A.; Nakatsuji, H.; Hada, M.; Ehara, M.; Toyota, K.; Fukuda, R.; Hasegawa, J.; Ishida, M.; Nakajima, T.; Honda, Y.; Kitao, O.; Nakai, H.; Klene, M.; Li, X.; Knox, J. E.; Hratchian, H. P.; Cross, J. B.; Adamo, C.; Jaramillo, J.; Gomperts, R.; Stratmann, R. E.; Yazyev, O.; Austin, A. J.; Cammi, R.; Pomelli, C.; Ochterski, J. W.; Ayala, P. Y.; Morokuma, K.; Voth, G. A.; Salvador, P.; Dannenberg, J. J.; Zakrzewski, V. G.; Dapprich, S.; Daniels, A. D.; Strain, M. C.; Farkas, O.; Malick, D. K.; Rabuck, A. D.; Raghavachari, K.; Foresman, J. B.; Ortiz, J. V.; Cui, Q.; Baboul, A. G.; Clifford, S.; Cioslowski, J.; Stefanov, B. B.; Liu, G.; Liashenko, A.; Piskorz, P.; Komaromi, I.; Martin, R. L.; Fox, D. J.; Keith, T.; Al-Laham, M. A.; Peng, C. Y.; Nanayakkara, A.; Challacombe, M.; Gill, P. M. W.; Johnson, B.; Chen, W.; Wong, M. W.; Gonzalez, C.; Pople, J. A. *Gaussian 03*, revision A.1; Gaussian, Inc.: Pittsburgh, PA, 2003.

(32) Schaftenaar, G.; Noordik, J. H. *J. Comput.-Aided Mol. Des.* **2000**, *14*, 123.

(33) Parr, R. G.; Yang, W. *Density-functional theory of atoms and molecules*; Oxford University Press: Oxford, U.K., 1989.

(34) Becke, A. D. *J. Chem. Phys.* **1993**, *98*, 5648.

(35) Perdew, J. P.; Chevary, J. A.; Vosko, S. H.; Jackson, K. A.; Pederson, M. R.; Singh, D. J.; Fiolhais, C. *Phys. Rev. B* **1992**, *46*, 6671.

(36) Cizek, J. *Adv. Chem. Phys.* **1969**, *14*, 35.

(37) Knowles, P. J.; Hampel, C.; Werner, H.-J. *J. Chem. Phys.* **1993**, *99*, 5219.

(38) Frisch, M. J.; Pople J. A.; Binkley, J. S. *J. Chem. Phys.* **1984**, *80*, 3265.

(39) Raghavachari, K.; Trucks, G. W.; Pople, J. A.; Head-Gordon, M. *Chem. Phys. Lett.* **1989**, *157*, 479.

(40) Clark, T.; Chandrasekhar, J.; Spitznagel, G. W.; Schleyer, P. v. R. *J. Comput. Chem.* **1983**, *4*, 294.

(41) McLean, A. D.; Chandler, G. S. *J. Chem. Phys.* **1980**, *72*, 5639.

(42) Bernardi, F.; Bottini, A.; McDougall, J. J. W.; Robb, M. A.; Schlegel, H. B. *Faraday Symp. Chem. Soc.* **1979**, *19*, 137.

(43) Frisch, M. J.; Ragazos, I. N.; Robb, M. A.; Schlegel, H. B. *Chem. Phys. Lett.* **1992**, *189*, 524.